



## Application of an R-group search technique in the molecular design of HIV-1 integrase inhibitors

JIAN-BO TONG\*, MIN BAI and XIANG ZHAO

College of Chemistry and Chemical Engineering, Shaanxi University of Science and Technology, Xi'an 710021, PR China

(Received 26 August, revised 29 November, accepted 30 November 2015)

**Abstract:** In this paper, a three-dimensional quantitative structure–activity relationship (3D-QSAR) study for 62 HIV-1 integrase (IN) inhibitors was established using Topomer CoMFA. The multiple correlation coefficient of fitting, cross-validation and external validation were 0.942, 0.670 and 0.748, respectively. The results indicated that the obtained Topomer CoMFA model had both favorable estimation stability and good prediction capability. Topomer Search was used to search the R group from the ZINC database. As a result, a series of R groups with a relatively high activity contribution was obtained. By filtering with the most potent molecule in the set, 1 Ra group and 21 Rb groups were selected. The 1 Ra groups and 21 Rb groups were employed to substitute alternately the Ra and Rb of sample **42**. Finally, 21 new compounds were designed and further their activities were predicted using the Topomer CoMFA model and there were 10 new compounds with higher activity than that of the template molecule. The results suggested the Topomer Search technology could be effectively used to screen and design new HIV-1 IN inhibitors and has good predictive capability to guide the design of new HIV/AIDS drugs.

**Keywords:** quantitative structure–activity relationship (QSAR); integrase inhibitors; Topomer CoMFA; Topomer Search; design of new inhibitors.

### INTRODUCTION

Acquired immunodeficiency syndrome (AIDS) caused by the human immunodeficiency virus (HIV) has been a threat to human health since it was first reported in 1981.<sup>1,2</sup> Anti-HIV drug development has been one of the leading tasks in the drug discovery area with the increase in the number of AIDS sufferers.<sup>3</sup> The inherent proteins involved in the viral replication cycle have been used as drug targets to design inhibitors to prevent the spread of infection, such as reverse transcriptase (RT), protease (PR), integrase (IN), glycoprotein (gp41 and gp120), as well as the host cell receptor (CD4) and co-receptor (CCR5 and CXCR4).<sup>4</sup>

\*Corresponding author. E-mail: jianbotong@aliyun.com  
doi: 10.2298/JSC150826003T

Twenty two drugs comprising reverse transcriptase inhibitors (RTI), protease inhibitors (PI) and entry inhibitors have been approved by the FDA for the treatment of HIV infection. Unfortunately, most of these drugs have produced different degrees of resistance. Hence, the research and development of new drugs has become an urgent priority Human immunodeficiency virus-1 (HIV-1) is characterized by reverse transcription of the viral RNA genome to cDNA and its integration into the host cell genome. Then, the integrated proviral DNA with a long terminal repeat (LTR) at each end is transcribed, leading to the synthesis of viral proteins and completion of the viral replication cycle. IN plays a pivotal role in virus replication. Moreover, IN is not present in the host cell but is in the virus itself and has no mammalian counterpart.<sup>5-7</sup> Thus, IN became an attractive and suitable target for the development of anti-AIDS drugs. HIV-1 IN is a 3'-*pol*-gene-encoded enzyme containing 288 amino acid residues.<sup>8,9</sup> HIV-1 IN comprises three domains: the *N*-terminal domain, the *C*-terminal domain and the catalytic domain. The catalytic domain contains a DDE motif (D64, D116 and E152) that forms metal chelating interactions with one or two divalent metal ions, such as Mn<sup>2+</sup> and Mg<sup>2+</sup>.<sup>10</sup> The whole process of the integration of HIV-1 cDNA into the chromosomes of the host cell by HIV-1 IN contains two steps: 3-processing and strand transfer. Raltegravir (RAL) became the first IN strand transfer inhibitor approved by the FDA in 2007.<sup>11,12</sup>

The availability of computational techniques on quantitative structure activity relationships (QSARs) might provide a potential direction for accelerating the process of drug design. In fact, QSAR could be viewed as a technique attempting to summarize chemical and biological information in a form that allows the generation of relationships between chemical structure and biological activity.<sup>13</sup> As is well known, the success of a QSAR study depends also on the selection of the variables (molecular descriptors) and on the representation of the information. Variables should give the maximum information in the activity variations. A 3D-QSAR model would better reflect the interactions between the ligand and receptor compared to a 2D-QSAR model. Comparative molecular field analysis (CoMFA)<sup>14</sup> is a method used widely in 3D-QSAR. In this paper, Topomer CoMFA,<sup>15,16</sup> the second generation of CoMFA, was employed to construct a 3D-QSAR model for 62 HIV-1 integrase inhibitors to analyze the chemical–biological interactions governing their activities toward HIV-1 IN. The Topomer CoMFA model could also be applied to conduct ligand-based virtual screening combining the Topomer Search<sup>17</sup> technology to lay the foundation of new drug design.

## PRINCIPLES AND METHODS

### *Data set*

In this study, the structures and experimental data of the 62 HIV-1 IN inhibitors obtained from the literature<sup>18</sup> are shown in Table I. The dataset was systematically divided into a

training set (45 compounds) and a test set (17 compounds). The number of compounds in the test set was approximately 30 % of those in the training set, which was considered as a proper ratio.<sup>19</sup> The training set was applied to build the 3D-QSAR model and the test set was used to verify the predictive ability of the model. The bioactivities of inhibitors are presented in pIC<sub>50</sub> (-log IC<sub>50</sub>). The IC<sub>50</sub> represents the concentration of an inhibitor that is required for 50 % intergrase inhibition.

TABLE I. Structures and bioactivities of the 62 integrase inhibitors

| No.                   | R <sub>1</sub>  | R <sub>2</sub> | R <sub>3</sub> | R <sub>4</sub> | R <sub>5</sub> | R <sub>6</sub>                                    | IC <sub>50</sub> / μM | Exp. pIC <sub>50</sub> | Pred. pIC <sub>50</sub> |
|-----------------------|-----------------|----------------|----------------|----------------|----------------|---|-----------------------|------------------------|-------------------------|
| <b>1</b>              | —               | —              | —              | —              | —              | —   | 0.05                  | 7.3010                 | 7.4712                  |
| <b>2<sup>a</sup></b>  | H               | H              | H              | H              | H              | H   | 1.63                  | 5.7878                 | 5.7911                  |
| <b>3</b>              | H               | H              | H              | H              | H              | CH <sub>3</sub>                                   | 2.30                  | 5.6383                 | 5.6374                  |
| <b>4</b>              | H               | Cl             | H              | H              | OH             | H   | 0.80                  | 6.0969                 | 6.2438                  |
| <b>5</b>              | Cl              | H              | H              | H              | OH             | H   | 0.41                  | 6.3872                 | 6.0375                  |
| <b>6<sup>a</sup></b>  | F               | H              | H              | H              | OH             | H   | 0.50                  | 6.3010                 | 6.3172                  |
| <b>7</b>              | Me              | H              | H              | H              | OH             | H   | 1.08                  | 5.9666                 | 5.9750                  |
| <b>8</b>              | OMe             | H              | H              | H              | OH             | H   | 1.17                  | 5.9318                 | 5.8369                  |
| <b>9</b>              | CF <sub>3</sub> | H              | H              | H              | OH             | H   | 0.72                  | 6.1427                 | 5.8379                  |
| <b>10</b>             | Cl              | H              | H              | Cl             | OH             | H   | 0.37                  | 6.4318                 | 6.4454                  |
| <b>11<sup>a</sup></b> | H               | Cl             | H              | Cl             | OH             | H   | 0.25                  | 6.6021                 | 6.2876                  |
| <b>12</b>             | Cl              | Cl             | H              | H              | OH             | H   | 0.07                  | 7.1549                 | 7.0814                  |
| <b>13</b>             | Cl              | Cl             | H              | H              | OH             | Me  | 0.083                 | 7.0809                 | 7.1392                  |
| <b>14<sup>a</sup></b> | Cl              | Cl             | H              | H              | OH             | Et  | 0.031                 | 7.5086                 | 7.3118                  |
| <b>15</b>             | Cl              | Cl             | H              | H              | OH             | Pr  | 0.055                 | 7.2596                 | 7.3060                  |
| <b>16</b>             | Cl              | Cl             | H              | H              | OH             | iPr   | 0.026                 | 7.5850                 | 7.4435                  |
| <b>17</b>             | Cl              | Cl             | H              | H              | OH             | Bu  | 0.065                 | 7.1871                 | 7.0327                  |
| <b>18<sup>a</sup></b> | Cl              | Cl             | H              | H              | OH             | CH <sub>2</sub> CO <sub>2</sub> H                 | 0.032                 | 7.4949                 | 7.4264                  |
| <b>19</b>             | Cl              | Cl             | H              | H              | OH             | (CH <sub>2</sub> ) <sub>2</sub> CO <sub>2</sub> H | 0.038                 | 7.4202                 | 7.3982                  |
| <b>20</b>             | Cl              | Cl             | H              | H              | OH             | CH <sub>2</sub> CONH <sub>2</sub>                 | 0.035                 | 7.4559                 | 7.4534                  |
| <b>21<sup>a</sup></b> | Cl              | Cl             | H              | H              | OH             | (CH <sub>2</sub> ) <sub>2</sub> CONH <sub>2</sub> | 0.116                 | 6.9355                 | 7.2167                  |
| <b>22</b>             | Cl              | Cl             | H              | H              | OH             | (CH <sub>2</sub> ) <sub>2</sub> NH <sub>2</sub>   | 0.215                 | 6.6676                 | 7.2085                  |
| <b>23</b>             | Cl              | Cl             | H              | H              | OH             | (CH <sub>2</sub> ) <sub>2</sub> OH                | 0.021                 | 7.6778                 | 7.4673                  |
| <b>24</b>             | Cl              | Cl             | H              | H              | OH             | (CH <sub>2</sub> ) <sub>3</sub> OH                | 0.077                 | 7.1135                 | 7.2954                  |
| <b>25<sup>a</sup></b> | Cl              | F              | H              | H              | OH             | (CH <sub>2</sub> ) <sub>2</sub> OH                | 0.044                 | 7.3565                 | 6.6186                  |
| <b>26</b>             | F               | Cl             | H              | H              | OH             | (CH <sub>2</sub> ) <sub>2</sub> OH                | 0.024                 | 7.6198                 | 7.8180                  |
| <b>27</b>             | Cl              | Cl             | H              | H              | F              | —   | 0.084                 | 7.0757                 | 7.0352                  |
| <b>28</b>             | Cl              | Cl             | F              | H              | H              | —   | 0.025                 | 7.6021                 | 7.6280                  |

TABLE I. Continued

| No.             | R <sub>1</sub> | R <sub>2</sub>                                  | R <sub>3</sub>  | R <sub>4</sub>  | R <sub>5</sub>   | R <sub>6</sub> | IC <sub>50</sub> / μM | Exp. pIC <sub>50</sub> | Pred. pIC <sub>50</sub> |
|-----------------|----------------|---|-----------------|-----------------|--|----------------|-----------------------|------------------------|-------------------------|
| 29              | Cl             | Cl  | H               | F               | H  | —              | 0.034                 | 7.4685                 | 7.4825                  |
| 30              | Cl             | Cl  | OMe             | H               | H  | —              | 0.012                 | 7.9208                 | 7.6462                  |
| 31 <sup>a</sup> | Cl             | Cl  | Cl              | H               | H  | —              | 0.043                 | 7.3665                 | 7.4009                  |
| 32              | Cl             | Cl  | Me              | H               | H  | —              | 0.041                 | 7.3872                 | 7.5342                  |
| 33 <sup>a</sup> | Cl             | Cl  | CF <sub>3</sub> | H               | H  | —              | 0.674                 | 6.1713                 | 6.9872                  |
| 34              | Cl             | Cl  | CN              | H               | H  | —              | 0.050                 | 7.3101                 | 7.4231                  |
| 35              | F              | Cl  | OMe             | H               | H  | —              | 0.009                 | 8.0458                 | 7.9970                  |
| 36              | H              | (S)-Me  | —               | —               | —  | —              | 0.0148                | 7.8297                 | 7.9084                  |
| 37              | H              | (R)-Me  | —               | —               | —  | —              | 0.0383                | 7.4168                 | 7.9076                  |
| 38 <sup>a</sup> | H              | (S)-Et  | —               | —               | —  | —              | 0.009                 | 8.0458                 | 7.9384                  |
| 39              | H              | (S)-Pr  | —               | —               | —  | —              | 0.0082                | 8.0862                 | 7.7193                  |
| 40 <sup>a</sup> | H              | (S)-iPr   | —               | —               | —  | —              | 0.0082                | 8.0862                 | 7.9061                  |
| 41              | H              | (S)-tBu   | —               | —               | —  | —              | 0.006                 | 8.2218                 | 7.9751                  |
| 42              | H              | (S)-cyclo-hexyl                                 | —               | —               | —  | —              | 0.0056                | 8.2518                 | 7.9954                  |
| 43              | H              | (S)-Ph  | —               | —               | —  | —              | 0.0098                | 8.0088                 | 8.0302                  |
| 44 <sup>a</sup> | OMe            | (S)-Pr  | —               | —               | —  | —              | 0.0058                | 8.2366                 | 7.8725                  |
| 45              | OMe            | (S)-iPr   | —               | —               | —  | —              | 0.0072                | 8.1427                 | 8.0813                  |
| 46              | OMe            | (R)-iPr   | —               | —               | —  | —              | 0.0144                | 7.8416                 | 7.6121                  |
| 47              | OMe            | (S)-tBu   | —               | —               | —  | —              | 0.0058                | 8.2366                 | 8.1655                  |
| 48 <sup>a</sup> | OMe            | (S)-cyclohexyl                                  | —               | —               | —  | —              | 0.0067                | 8.1739                 | 8.1191                  |
| 49              | —              | —   | —               | —               | —  | —              | 9                     | 5.0458                 | 5.1364                  |
| 50              | Bn             | CH <sub>3</sub>                                 | —               | —               | —  | —              | 6                     | 5.2218                 | 5.2892                  |
| 51 <sup>a</sup> | 4-F-Bn         | CH <sub>3</sub>                                 | —               | —               | —  | —              | 0.9                   | 6.0458                 | 5.2451                  |
| 52              | OPh            | CH <sub>3</sub>                                 | —               | —               | —  | —              | 14                    | 4.8539                 | 4.7144                  |
| 53 <sup>a</sup> | 4-F-Bn         | (CH <sub>2</sub> ) <sub>4</sub> CH <sub>3</sub> | —               | —               | —  | —              | 5                     | 5.3010                 | 4.8765                  |
| 54              | H              | H   | H               | S               | (CH <sub>2</sub> ) <sub>2</sub> OH                                     | —              | 18.5                  | 4.7328                 | 4.7834                  |
| 55              | Cl             | H   | Cl              | CH <sub>2</sub> | (CH <sub>2</sub> ) <sub>2</sub> OH                                     | —              | 0.2                   | 6.6990                 | 5.8825                  |
| 56              | Cl             | H   | Cl              | CH <sub>2</sub> | (CH <sub>2</sub> ) <sub>3</sub> OH                                     | —              | 1.3                   | 5.8861                 | 5.7093                  |
| 57 <sup>a</sup> | Cl             | H   | Cl              | CH <sub>2</sub> | (CH <sub>2</sub> ) <sub>4</sub> OH                                     | —              | 0.6                   | 6.2218                 | 5.9280                  |
| 58              | Cl             | H   | Cl              | CH <sub>2</sub> | (CH <sub>2</sub> ) <sub>2</sub> N—<br>—(CH <sub>3</sub> ) <sub>2</sub> | —              | 24.1                  | 4.6180                 | 5.1304                  |
| 59              | Cl             | H   | Cl              | CH <sub>2</sub> | (CH <sub>2</sub> ) <sub>2</sub> O—<br>—CH <sub>3</sub>                 | —              | 16.5                  | 4.7825                 | 5.4701                  |
| 60              | F              | Cl  | NH              | —               | —  | —              | 2.1                   | 5.6778                 | 5.5582                  |
| 61 <sup>a</sup> | H              | H   | S               | —               | —  | —              | 1.6                   | 5.7959                 | 6.7275                  |
| 62              | —              | —   | —               | —               | —  | —              | 0.0435                | 7.3615                 | 7.4321                  |

<sup>a</sup>Chosen as the test set*Molecular structure construction*

The 3D structures of 62 HIV-1 IN inhibitors were constructed using the sketch module of the Sybyl 2.0-X package. All molecules were optimized using the tripos force field and the gradient descent method with an energy change of 0.005 kcal\* mol<sup>-1</sup>. Partial charges for all the molecules were added using the Gasteiger-Hückel method. The maximum iteration number was 1000. The other parameters were defaulted by Sybyl 2.0-X.

\* 1kcal = 4186 J

### *Topomer CoMFA modeling*

Topomer CoMFA is a rapid fragment-based 3D-QSAR method to predict significant R-groups of molecules. The Topomer CoMFA method identifies bioactivity values with the help of a compound library as a source with automated rules.<sup>14</sup> The process of standard Topomer CoMFA is completed by the following two steps: the first step is the generation of the Topomer 3D models for each fragment of the molecule. Topomer CoMFA divides one compound into two or more fragments. By confirming how to break down the structure of compounds, the Topomer CoMFA can automatically identify the features and charges of the fragments.<sup>20</sup> The second step consists of performing CoMFA with partial least squares (PLS) using leave-one-out (LOO) cross-validation in order to form a predictive model.<sup>21</sup> During the process of building the model, the CoMFA method is used to deal with the large amounts of data. By objective measures and automatic matching to analyze the characters of compounds, Topomer CoMFA is more efficient in forming predictive models compared with CoMFA.

In the process of Topomer CoMFA, the measure of fracture could affect the quality of the model. In this study, the structure of each of the training set was broken into two sets of fragments, shown as Ra (blue) and Rb (red) groups as presented in Fig. 1. Initially, as it had the highest activity, molecule **42** was selected as the template molecule. Based on compound **42**, the cutting style was confirmed. The molecule was cut to obtain the Ra group and the Rb group. Other training molecules were identified automatically and cut in this style. The molecules not identified required manual cutting. Then the steric and electrostatic field energy between the molecules was calculated. The descriptors obtained were considered as the independent variables and the  $\text{pIC}_{50}$  values were regarded as the dependent variables in partial least square (PLS)<sup>22</sup> to build the Topomer CoMFA model. The model was evaluated by the leave-one-out cross-validation (LOO-CV) approach. The test molecules were predicted by the Topomer CoMFA model to verify the predictive ability of the obtained model.

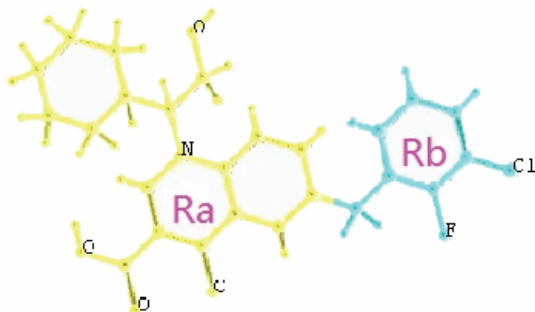


Fig. 1. Cutting style of molecule **42**.

### *Molecular screening*

Molecular screening was realized using the Topomer Search technology, a fast 3D ligand-based virtual screening tool. The principle is explained as following: the molecules in the database are cut into fragments, which are compared with the Topomer similarity of the R groups of the training molecules. Then the Topomer CoMFA model is used to predict their contributions to their activity. Finally, a series of R groups is obtained. In this study, Topomer Search was employed to search R groups with relatively high activity contributions from

drug-like in the ZINC (2012) database (130,000 compounds). The Topomer distance was set as 185 to evaluate the binding degree, and other parameters were defaulted by Sybyl 2.0-X.

## RESULTS AND DISCUSSION

### *Topomer CoMFA modeling results and evaluation*

To generate statistically significant 3D-QSAR models, the ligand-based alignment rule was used. In this study, regression analysis was performed using the partial least squares (PLS) method.<sup>23</sup> Some statistical parameters were used to analyze the stand or fall of these models, including the cross-validated coefficient ( $q^2$ ), the standard deviation of error prediction ( $r^2$ ), standard error of estimate ( $SEE$ ) and  $F$ -statistic values. A high  $q^2$  and  $r^2$  value ( $q^2 > 0.5$ ,  $r^2 > 0.6$ ) is considered as a proof of a high predictive ability of a model.<sup>24</sup> The statistical results of the model in this study are displayed in Table II, from which it could be seen that the  $q^2$  value was 0.670, an optimized component of 6 and the  $r^2$  value was 0.942, which suggested that the model also has predictive ability ( $q^2 > 0.5$ ). The  $pIC_{50}$  value of the test set was predicted with a  $q_{pred}^2$  value of 0.748. The linear regression between the experimental  $pIC_{50}$  and the predicted  $pIC_{50}$  for the training set and test set are shown in Fig. 2. The predicted bioactivities ( $pIC_{50}$ ) for the training set and test set are given in Table I. The results indicate that the model has both favorable estimation stability and good prediction capabilities.

TABLE II. The statistical results of Topomer CoMFA;  $N$  – optimal components,  $r^2$  – the multiple correlation coefficient of fitting,  $q^2$  – the multiple correlation coefficient of cross validation,  $q_{pred}^2$  – the multiple correlation coefficient of external validation,  $SEE$  – standard estimated error,  $SD$  – fitting standard deviation,  $SD_{CV}$  – cross-validation standard deviation,  $F$  – Fisher value

| Statistical parameter | $N$ | $r^2$ | $q^2$ | $q_{pred}^2$ | $SEE$ | $SD$ | $SD_{CV}$ | $F$     |
|-----------------------|-----|-------|-------|--------------|-------|------|-----------|---------|
| Topomer CoMFA         | 6   | 0.942 | 0.670 | 0.748        | 0.277 | 0.28 | 0.67      | 103.344 |

Lu, Wei and Zhang performed a 3D-QSAR analysis on a series of quinoline carboxylic derivatives of HIV-1 intergrase inhibitors using the CoMFA and CoMSIA method.<sup>25</sup> Compared with the present study, they entered more molecular structures into the analysis. In the present study, a fair result ( $q^2 = 0.670$ ,  $r^2 = 0.942$ ,  $SEE = 0.277$ ,  $F = 103.344$ ) was achieved with Topomer CoMFA models. These results mean that the predictive models have a wider range of application and similar or even better molecular structure prediction than the former work. Furthermore, the introduction of Topomer CoMFA provides a brand new method to analyze substitution of a functional group rather than of a functional atom. In addition, by objective measures and automatic matching to analyze characters of compounds, Topomer CoMFA is more efficient in forming predictive models. Hence, the work performed herein has practical meaning and far-reaching influence.

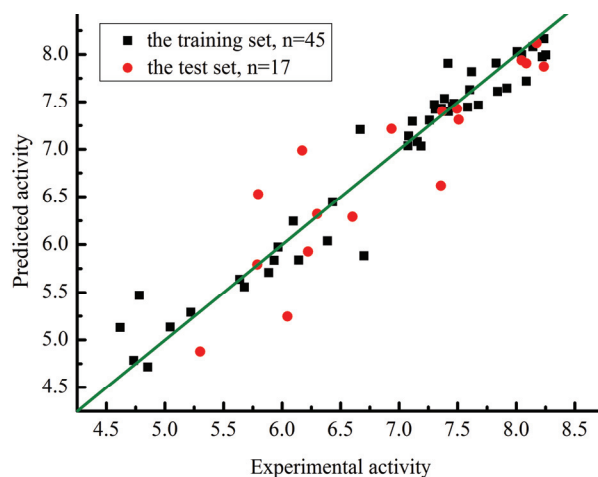


Fig. 2. Linear regression between experimental and predicted  $\text{pIC}_{50}$  values of 62 inhibitors.

### 3D contour plots of the Topomer CoMFA model

The three-dimensional contour plots of the Topomer CoMFA model are shown in Fig. 3a–d with the sample **42** as the reference structure. The contour

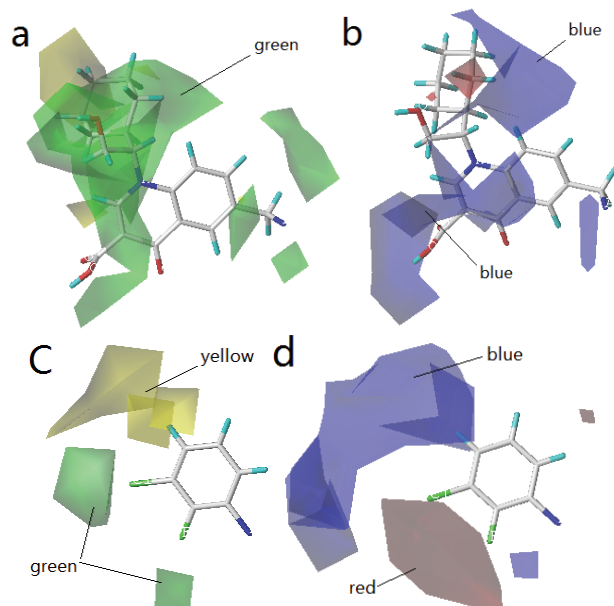


Fig. 3. 3D contour of Topomer CoMFA model: a) steric field map of Ra; b) electrostatic field map of Ra; c) steric field map of Rb; d) electrostatic field map of Rb (green and yellow contours represent steric favorable and unfavorable regions, respectively. Blue and red contours represent regions that favor electropositive and electronegative groups, respectively).

maps provide information on factors affecting the activities of the molecules. This is particularly important when increasing or reducing the activity of a compound by changing its molecular structure. The steric interaction of the Ra and Rb groups is represented by green and yellow contours in Fig. 3a and c, respectively, while the electrostatic interaction of the Ra and Rb groups is denoted by red and blue contours in Fig. 3b and d, respectively. The green contours represent regions where a large or bulky substituent is favorable for the activity. The opposite is true for the yellow contours. The red isopleths indicate regions where a negatively charged substituent is favorable for the activity and the blue isopleths indicate regions where an increase of a positive charge of substituent enhances the activity.

As shown in Fig. 3a, a green contour covering the cyclohexyl group linked to R<sub>2</sub> indicates the presence of a bulky group is good for the biological activity. This is in agreement with the experimental data: **38** (-Et) > **37** (-Me), **41** (-tBu) > **40** (-iPr). Molecule **42** has the highest activity because of the bulky substituent (-cyclohexyl) at the R<sub>2</sub>-position. Moreover, the green contour near the R<sub>2</sub>-position of the molecule **42** indicates the bulky substituent in this position may be favorable for the activity. For example, molecule **45** (-OMe) has a higher activity than molecule **40** (-H). According to Fig. 3b, there is a large blue contour around cyclohexyl (R<sub>2</sub>), which suggests that a positively charged substituent at R<sub>2</sub>-position may favor the activity. This is in agreement with the experimental data: **39** (-Pr), **40** (-iPr), **41** (-tBu) and **42** (-cyclohexyl). In Fig. 3c and d, a yellow and a large blue contour at the 4-position of the phenyl ring indicate that a small and positively charged substituent is preferred in this region. A red contour at the 2- and 3-position of the phenyl ring in Fig. 3d, suggests the introduction of an electronegative substituent at this position would be of benefit for inhibitory activity. It can show the fact that the -Cl and -F have been introduced in this position.

#### *Molecular screening and molecular design*

The results of the molecular screening using the Topomer search technology were evaluated by the Topomer distance (TOPDIST) and the contribution values of R-groups (TOPCOMFA\_R). Under normal circumstances, priority was given to TOPCOMFA\_R in the same limit of the TOPDIST. In this study, 5000 Ra groups and 1000 Rb groups were screened from drug-like in the ZINC (2012) database. 1 Ra group and 21 Rb groups with higher TOPCOMFA\_R than that of template molecule were selected from 5000 Ra groups and 1000 Rb groups.

The 1 Ra group and 21 Rb groups were employed to substitute alternately for the Ra and Rb of sample **42** and 21 new molecules were designed. All molecules were optimized using the method applied to the training molecules and further their activities were predicted using the obtained Topomer CoMFA model. The structures and predicted activities of the 21 new compounds are displayed in

Table III, from which could be seen that there are 10 new compounds with higher activity than that of the template molecule. Furthermore, as revealed in Table III, 10 new compounds had higher activities because of the introduction of an electronegative substituent into 2- and 3-position of the phenyl ring of Rb. Moreover, bulky substituents in Ra contribute to the activity of 10 new compounds. This is consistent with the analysis of the 3D contour of the Topomer CoMFA model.

TABLE III. Structures and predicted  $pIC_{50}$  values of new designed molecules

| Cmpd.          | Structure | Pred.  | Cmpd.          | Structure | Pred.  |
|----------------|-----------|--------|----------------|-----------|--------|
| a <sup>a</sup> |           | 8.2652 | I <sup>a</sup> |           | 8.2761 |
| b              |           | 8.0578 | m              |           | 8.0433 |
| c <sup>a</sup> |           | 8.6310 | n <sup>a</sup> |           | 8.6773 |
| d <sup>a</sup> |           | 8.3685 | o              |           | 8.1185 |
| e <sup>a</sup> |           | 8.3283 | p              |           | 8.1452 |
| f <sup>a</sup> |           | 8.3148 | q <sup>a</sup> |           | 8.8139 |

TABLE III. Continued

| Cmpd.                | Structure | Pred.  | Cmpd.                | Structure | Pred.  |
|----------------------|-----------|--------|----------------------|-----------|--------|
| <b>g</b>             |           | 7.8841 | <b>r</b>             |           | 8.0917 |
| <b>h</b>             |           | 7.7815 | <b>s<sup>a</sup></b> |           | 8.4089 |
| <b>i<sup>a</sup></b> |           | 8.4612 | <b>t</b>             |           | 7.9982 |
| <b>j</b>             |           | 8.1987 | <b>u</b>             |           | 8.0043 |
| <b>k</b>             |           | 8.1189 |                      |           |        |

<sup>a</sup>Compounds with higher activity than that of the template molecule

## CONCLUSIONS

In the present work, 62 HIV-1 IN inhibitors were studied by computer-aided drug design processes, *i.e.*, 3D-QSAR/Topomer CoMFA studies. The model was favored by internal and external predictions and the statistics were convincing and comparable. The model could not only be extrapolated to predict novel and more potent inhibitors, but also the contour maps obtained from Topomer CoMFA analyses provide a useful insight for structure-based design of new chemical entities with high HIV-1 inhibitory activity. This study could serve as a basis for the development of HIV-1 IN inhibitors.

*Acknowledgments.* We gratefully acknowledge support of this research by the basic research project of Natural Science of Shaanxi Province (2015JM2057) and the Graduate Innovation Fund of Shaanxi University of Science and Technology.

## ИЗВОД

ПРИМЕНА ТЕХНИКЕ ПРЕТРАГЕ R-ГРУПЕ НА МОЛЕКУЛСКИ ДИЗАЈН ИНХИБИТОРА  
HIV-1 ИНТЕГРАЗЕ

JIAN-BO TONG, MIN BAI и XIANG ZHAO

*College of Chemistry and Chemical Engineering, Shaanxi University of Science & Technology, Xi'an 710021, China*

У овом раду је установљена квантитативна релација тродимензионалне структуре и активности (3D-QSAR) проучавањем 62 инхибитора HIV-1 интегразе (IN), коришћењем методе Topomer CoMFA. Кофицијенти вишеструке корелације фитовања, унакрсне валидације и екстерне валидације били су 0,942, 0,670, односно 0,748. Ови резултати указују да добијени Topomer CoMFA модел има и повољну стабилност за процењивање и добру способност предвиђања. Topomer Search био је коришћен за претрагу ZINC базе података на R групу. Као резултат, добијен је низ R група са великим доприносом активности. Филтрирањем преко најпотентнијег молекула у скупу, изабране су 1 Ra група и 21 Rb група. Употребили смо 1 Ra групу и 21 Rb групу да замене Ra и Rb у узорку **42**. Коначно, дизајнирали смо 21 ново једињење и затим предсказали њихове активности користећи Topomer CoMFA модел и нашли 10 нових једињења са активношћу већом него прототипни молекул. Резултати сугеришу да се техника Topomer Search може ефикасно користити за скрининг и дизајн нових инхибитора HIV-1 IN, и да има добру способност предвиђања за дизајн нових HIV/AIDS лекова.

(Примљено 26. августа, ревидирано 29. новембра, прихваћено 30. новембра 2015)

## REFERENCES

1. A. S. Fauci, *Science* **239** (1998) 617
2. F. J. Palella Jr., K. M. Delaney, A. C. Moorman, M. O. Loveless, J. Fuhrer, G. A. Satten, D. J. Aschman, S. D. Holmberg, *N. Engl. J. Med.* **338** (1998) 853
3. R. V. Patel, Y. S. Keum, S. W. Park, *Eur. J. Med. Chem.* **97** (2015) 649
4. J. P. Moore, S. G. Kitchen, P. Pugach, J. A. Zack, *AIDS Res. Hum. Retroviruses* **20** (2004) 111
5. J. L. Blanco, G. Whitlock, A. Milinkovic, G. Moyle, *Expert Opin. Pharmacother.* **16** (2015) 1313
6. R. Craigie, *J. Biol. Chem.* **276** (2001) 23213
7. W. G. Powderly, *J. Antimicrob. Chemother.* **65** (2010) 2485
8. D. Esposito, R. Craigie, *Adv. Virus Res.* **52** (1999) 319
9. D. J. Hazuda, *Braz. J. Infect. Dis.* **14** (2010) 513
10. Y. Goldgur, F. Dyda, A. B. Hickman, T. M. Jenkins, R. Craigie, R. D. Davies, *Proc. Natl. Acad. Sci. USA* **95** (1998) 9150
11. S. Ray, Z. Fatima, A. Saxena, *Mini-Rev. Med. Chem.* **10** (2010) 147
12. V. Summa, A. Petrocchi, F. Bonelli, B. Crescenzi, M. Donghi, M. Ferrara, F. Fiore, C. Gardelli, O. G. Paz, D. J. Hazuda, P. Jones, O. Kinzel, R. Laufer, E. Monteagudo, E. Muraglia, E. Nizi, F. Orvieto, P. Pace, G. Pescatore, R. Scarpelli, K. Stillmock, M. V. Witmer, M. Rowley, *J. Med. Chem.* **51** (2008) 5843
13. J. B. Tong, *PhD Thesis*, Shanxi University, Taiyuan, 2007
14. R. D. Cramer, *J. Med. Chem.* **46** (2003) 374
15. R. D. Cramer, D. E. Patterson, J. D. Bunce, *J. Am. Chem. Soc.* **110** (1988) 5959
16. R. D. Cramer, P. Cruz, G. Stahl, W. C. Curtiss, B. Campbell, B. B. Masek, F. Soltanshahi, *J. Chem. Inf. Model.* **48** (2008) 2180

17. R. D. Cramer, F. Soltanshahi, R. Jilek, B. Campbell, *J. Comput.-Aided Mol. Des.* **21** (2007) 341
18. Z. J. Cheng, Y. Zhang, W. Z. Fu, *Eur. J. Med. Chem.* **45** (2010) 3970
19. E. Cichero, S. Cesarin, L. Mosti, P. Fossa, *J. Mol. Model.* **16** (2010) 1481
20. A. Golbraikh, A. Tropsha, *J. Mol. Graphics Modell.* **20** (2002) 269
21. M. Le Bret, J. Polanski, F. Zouhiri, L. Jeanson, D. Desmaele, J. d'Angelo, J. F. Mouscadet, R. Gieleciak, J. Gasteiger, *J. Med. Chem.* **45** (2002) 4647
22. L. Xu, X. G. Shao, *Methods of Chemometrics*. Science Press, Beijing, 2004, p. 166
23. L. Stähle, S. Wold, *J. Chemom.* **1** (1987) 185
24. P. P. Roy, J. T. Leonard, K. Roy, *Chemom. Intell. Lab. Syst.* **90** (2008) 31
25. P. Lu, X. Wei, R. S. Zhang, *Eur. J. Med. Chem.* **45** (2010) 3413.